

RNA Helicase DEAD Box Protein 5 Regulates Polycomb Repressive Complex 2/Hox Transcript Antisense Intergenic RNA Function in Hepatitis B Virus Infection and Hepatocarcinogenesis

Hao Zhang,^{1,2} Zheng Xing,^{2,3} Saravana Kumar Kailasam Mani,^{1,2} Brigitte Bancel,⁴ David Durantel,⁴ Fabien Zoulim,⁴ Elizabeth J. Tran,^{2,3} Philippe Merle,⁴ and Ourania Andrisani^{1,2}

Chronic hepatitis B virus (HBV) infection is a major factor in hepatocellular carcinoma (HCC) pathogenesis by a mechanism not yet understood. Elucidating mechanisms of HBV-mediated hepatocarcinogenesis is needed to gain insights into classification and treatment of HCC. In HBV replicating cells, including virus-associated HCCs, suppressor of zeste 12 homolog (SUZ12), a core subunit of Polycomb repressive complex2 (PRC2), undergoes proteasomal degradation. This process requires the long noncoding RNA, Hox transcript antisense intergenic RNA (HOTAIR). Intriguingly, HOTAIR interacts with PRC2 and also binds RNA-binding E3 ligases, serving as a ubiquitination scaffold. Herein, we identified the RNA helicase, DEAD box protein 5 (DDX5), as a regulator of SUZ12 stability and PRC2-mediated gene repression, acting by regulating RNA-protein complexes formed with HOTAIR. Specifically, knockdown of DDX5 and/or HOTAIR enabled reexpression of PRC2-repressed genes epithelial cell adhesion molecule (EPCAM) and pluripotency genes. Also, knockdown of DDX5 enhanced transcription from the HBV minichromosome. The helicase activity of DDX5 stabilized SUZ12- and PRC2-mediated gene silencing, by displacing the RNA-binding E3 ligase, Mex-3 RNA-binding family member B (Mex3b), from HOTAIR. Conversely, ectopic expression of Mex3b ubiquitinated SUZ12, displaced DDX5 from HOTAIR, and induced SUZ12 down-regulation. In G₂ phase of cells expressing the HBV X protein (HBx), SUZ12 preferentially associated with Mex3b, but not DDX5, resulting in de-repression of PRC2 targets, including EPCAM and pluripotency genes. Significantly, liver tumors from HBx/c-myc bistransgenic mice and chronically HBV-infected patients exhibited a strong negative correlation between DDX5 messenger RNA levels, pluripotency gene expression, and liver tumor differentiation. Notably, chronically infected HBV patients with HCC expressing reduced DDX5 exhibited poor prognosis after tumor resection, identifying DDX5 as an important player in poor prognosis HCC. **Conclusion:** The RNA helicase DDX5, and E3 ligase Mex3b, are important cellular targets for the design of novel, epigenetic therapies to combat HBV infection and poor prognosis HBV-associated liver cancer. (HEPATOLOGY 2016;64:1033-1048)

Abbreviations: Abs, antibodies; ATP, adenosine triphosphate; cDNA, complementary DNA; cccDNA, circular covalently closed DNA; ChIP, chromatin immunoprecipitation; CHX, cyclohexamide; DDX5, DEAD box protein 5; DTT, dithiothreitol; Dzip3, DAZ-interacting zinc finger protein 3; dTB, double thymidine block; EED, embryonic ectoderm development; ELISA, enzyme-linked immunosorbent assay; EPCAM, epithelial cell adhesion molecule; ESCs, embryonic stem cells; FA, fluorescent anisotropy; H3K27me3, trimethylation of H3 on K27; HBc, HBV core; HBeAg, HBe antigen; HBV, hepatitis B virus; HBx, HBV X protein; HCC, hepatocellular carcinoma; hCSCs, hepatic cancer stem cells; HOTAIR, Hox transcript antisense intergenic RNA; IGFII, insulin-like growth factor II; IgG, immunoglobulin G; lncRNA, long noncoding RNA; Mex3b, Mex-3 RNA-binding family member B; mRNA, messenger RNA; NTCP, sodium taurocholate cotransporting peptide; OCT4, octamer 4; pgRNA, pregenomic RNA; PHHs, primary human hepatocytes; PLK1, polo-like-kinase 1; PRC2, Polycomb repressive complex 2; qPCR, quantitative PCR; RIP, ribonucleoprotein immunoprecipitation; RNP, RNA-protein; RT-PCR, reverse-transcriptase polymerase chain reaction; siRNA, small interfering RNA; SOX2, SRY (sex determining region Y)-box 2; SUZ12, suppressor of zeste 12 homolog; WCE, whole-cell extracts; WT, wild type.

Received May 2, 2016; accepted June 13, 2016.

Additional Supporting Information may be found at onlinelibrary.wiley.com/doi/10.1002/hep.28698/supinfo.

Chronic hepatitis B virus (HBV) infection is a major factor in development of hepatocellular carcinoma (HCC),⁽¹⁾ and the 16.5-kDa HBV X protein (HBx) protein encoded by HBV is a cofactor in HCC pathogenesis.^(2,3) Despite the HBV vaccine, the World Health Organization estimates that 250 million people globally are chronically infected with HBV. Moreover, the HBV vaccine is not always protective; children born of infected mothers become chronically infected. Current treatments include antiviral nucleoside analogs, efficient in suppressing HBV replication, but having no impact on persistence of the viral minichromosome, or production of the HBV oncoprotein HBx by the integrated viral DNA.⁽⁴⁾ In advanced-stage HCC, sorafenib therapy provides survival improvement, delaying tumor progression.^(5,6) Thus, new and effective mechanism-based therapies are needed to inhibit deleterious effects of HBx protein on cell homeostasis, by targeting essential mechanisms of viral replication and HCC pathogenesis.

Herein, we have identified such a molecular mechanism, having a role both in HBV replication and hepatocarcinogenesis. It involves the RNA helicase, DEAD box protein 5 (DDX5), regulating stability and function of the chromatin modifying Polycomb repressive complex 2 (PRC2). Suppressor of zeste 12 homolog (SUZ12), an essential subunit of PRC2, is down-regulated in HBV-replicating cells and liver tumors of animals modeling HBV-induced liver cancer.^(7,8) SUZ12 down-regulation involves proteasomal degradation initiated by

phosphorylation of SUZ12 by mitotic polo-like-kinase 1 (PLK1),⁽⁹⁾ which is activated by HBx.⁽¹⁰⁾ Intriguingly, SUZ12 degradation is accelerated by the long noncoding RNA (lncRNA), Hox transcript antisense intergenic RNA (HOTAIR),⁽⁹⁾ suggesting that the E3 ligase that ubiquitinates SUZ12 also binds to HOTAIR.

The PRC2 complex regulates lineage selection during embryonic development and stem cell differentiation^(11,12) by trimethylation of H3 on K27 (H3K27me3), a transcription silencing modification. PRC2 associates with more than 9,000 lncRNAs^(13,14) and represses transcription of >1,000 genes in embryonic stem cells (ESCs).⁽¹¹⁾ lncRNAs are proposed to recruit PRC2 to specific gene loci for repression through direct protein-RNA interactions.^(15,16) However, neither association with chromatin nor with RNA is sufficient for gene repression.^(17,18) Specific gene repression may require active remodeling of PRC2-lncRNA complexes by RNA helicases.⁽¹⁹⁾ One family of RNA helicases is the DEAD box helicases, which function as RNA-dependent ATPases and adenosine triphosphate (ATP)-dependent RNA helicases,^(20,21) unwinding RNA duplexes, displacing proteins from RNA, and remodeling RNA-protein (RNP) complexes.^(20,21)

Here, we provide evidence that SUZ12 interacts with DEAD box RNA helicase DDX5/p68.⁽²²⁾ Mammalian DDX5 acts as a transcriptional regulator⁽²²⁾ by associating with different transcriptional effectors.^(23,24) The yeast homolog of DDX5 functions in lncRNA-dependent

This work was supported by NIH grant DK044533 (to O.A.), GM097332-01 (to E.J.T.), and French grants PAIR-CHC 2009 (contract #2009-143, project ENELIVI) from Institut National du Cancer (INCa; to P.M.). Shared Resources (flow cytometry and DNA sequencing) are supported by NIH grant P30CA023168 to Purdue Center for Cancer Research and NIH/NCRR RR025761.

Copyright © 2016 The Authors. HEPATOLOGY published by Wiley Periodicals, Inc., on behalf of the American Association for the Study of Liver Diseases. This is an open access article under the terms of the Creative Commons Attribution-NonCommercial-NoDerivs License, which permits use and distribution in any medium, provided the original work is properly cited, the use is non-commercial and no modifications or adaptations are made. [The copyright line for this article was changed on October 27, 2016, after original online publication.]

View this article online at wileyonlinelibrary.com.

DOI 10.1002/hep.28698

Potential conflict of interest: Nothing to report.

ARTICLE INFORMATION:

From the ¹Department of Basic Medical Sciences, ²Purdue Center for Cancer Research, and ³Department of Biochemistry, Purdue University, West Lafayette, IN; ⁴Center for Cancer Research of Lyon, UMR INSERM 1052, CNRS 5286, Lyon Cedex 03, France.

ADDRESS CORRESPONDENCE AND REPRINT REQUESTS TO:

Ourania Andrisani, Ph.D.
Purdue University
205 Hansen Building
201 South University Street

West Lafayette, IN 47907
Tel: + 1-765-494-8131
E-mail: andrisao@purdue.edu

gene regulation,⁽²⁵⁻²⁸⁾ supporting that DEAD box RNA helicases can influence lncRNA function *in vivo*. Here, we show that DDX5 has a role in RNP complexes formed with HOTAIR. HOTAIR binds to PRC2 complex and represses transcription of specific genes⁽²⁹⁾ and also associates with RNA-binding E3 ligases, serving as a ubiquitination scaffold.⁽³⁰⁾

In this study, we dissected the role of RNA helicase DDX5 in PRC2-mediated repression of transcription both of cellular genes and the HBV minichromosome.⁽³¹⁾ Histone modifications of the viral minichromosome determine the rate of viral transcription and, in turn, the rate of viral replication.⁽³²⁾ We provide evidence that DDX5, by regulating PRC2 stability and function, has a dual role in infected hepatocytes; namely, regulation of HBV replication, and expression of specific host genes involved in HBV-mediated hepatocarcinogenesis. These genes include epithelial cell adhesion molecule (EpCAM) and pluripotency genes expressed in hepatic cancer stem cells (hCSCs).^(33,34) Importantly, analyses of DDX5 expression in liver tumors from X/c-myc bitransgenic mice⁽²⁾ and chronically HBV-infected patients identify DDX5 as an important molecule in pathogenesis of poor prognosis HBV-mediated liver cancer.

Materials and Methods

CELL CULTURE, TRANSFECTIONS, PLASMIDS, SMALL INTERFERING RNAs AND SYNCHRONIZATION PROTOCOLS

HEK293T, HepG2 cells, and mouse hepatocyte AML12 cell lines were purchased from ATCC, Manassas, VA. Tetracycline regulated HBx-expressing 4pX-1 cells, derived from AML12 cell line, were grown as described,⁽³⁵⁾ with tetracycline (5 $\mu\text{g}/\text{mL}$) or without tetracycline for 16-18 hours to allow HBx expression. HBx expression was confirmed by reverse-transcriptase polymerase chain reaction (RT-PCR). Synchronization of 4pX-1 cells in G₁/S by double thymidine block (dTb) was as described.⁽¹⁰⁾ Transient transfections used Lipofectamine 2000 (Invitrogen, Carlsbad, CA), with 2 μg each of the following plasmids: pcDNA empty vector, pcDNA-DDX5-D248N-Flag, pcDNA-DDX5-K149N-Flag, pcDNA-DDX5-Flag, SUZ12-HA, Plk1^{CA}-GFP, Ubiquitin-FLAG, and pcDNA3-HOTAIR.⁽²²⁾ Small interfering RNAs (siRNAs) for DDX5, Mex-3 RNA-binding family member B (Mex3b), and scrambled control siRNA (siCtrl) were

transfected using Lipofectamine RNAiMAX (Invitrogen). Cell lines were routinely tested for mycoplasma.

BIOCHEMICAL ATPase ASSAYS

In vitro ATP hydrolysis assays were performed using an enzyme-coupled absorbance assay.⁽³⁶⁾ ATP hydrolysis rate was measured using 400 nM of purified, recombinant MBP-DDX5-GST, or mutants in the presence and absence of 250 $\mu\text{g}/\text{mL}$ of total yeast RNA (Sigma-Aldrich, St. Louis, MO). k_{obs} values were calculated using the formula: $V_0 = (A_{340}/\text{min} \times 2.5)/(6.22 \times 10^{-3} \mu\text{M})$, where $k_{\text{obs}}(\text{min}^{-1}) = V_0/\text{protein concentration}$. DDX5 fused to an N-terminal MBP and C-terminal GST tag (MBP-DDX5-GST) was expressed in *Escherichia coli* and purified by affinity chromatography. DDX5 mutants were purified by the same method (N = 3; error bars represent SD).

FLUORESCENCE ANISOTROPY ASSAY

5'-FAM-labeled RNA 5'-AGCACCGUAAAGA CGC-3' was purchased from IDT (Integrated DNA Technologies, Coralville, IA). Reaction mixtures (40 μL) contained 40 mM of Tris-HCl (pH 8.0), 30 mM of NaCl, 2.5 mM of MgCl₂, 2 mM of 5'-adenylylimidodiphosphate, 2 mM of dithiothreitol (DTT), 40 U of Superase-in (Life Technologies, Carlsbad, CA), 10 nM of fluorescent RNA, and purified recombinant proteins. Binding reactions were incubated at 25 °C for 30 minutes, and assays were performed in black 96-well microplates (Corning Incorporated, Corning, NY, #3686) by measuring fluorescence anisotropy (FA) signals of 6-FAM ($\lambda_{\text{ex}} = 495 \text{ nm}$ and $\lambda_{\text{em}} = 520 \text{ nm}$) utilizing a BioTek Synergy 4 plate reader. Data were fitted to $Y = B_{\text{max}}^* X / (K_d + X)$ equation.

RIBONUCLEOPROTEIN IMMUNOPRECIPITATION ASSAYS

Ribonucleoprotein immunoprecipitation (RIP) were performed as described.⁽³⁰⁾ Whole-cell extracts (WCE) prepared in lysis buffer (Cell Signaling Technology, Danvers, MA) were incubated on ice for 30 minutes, followed by centrifugation at 10,000g for 15 minutes at 4 °C. Supernatants were incubated with antibodies for DDX5 (Millipore, Temecula, CA), Mex3b (Santa Cruz Biotechnology, Dallas, TX), or control immunoglobulin G (IgG; Cell Signaling Technology) for 1 hour at 4 °C, followed by addition of protein A/G beads (40 μL) and

overnight incubation at 4°C. Beads were washed with RIP buffer (150 mM of KCl, 25 mM of Tris [pH 7.4], 5 mM of ethylenediaminetetraacetic acid, 0.5 mM DTT, and 0.5% NP-40), complexes were treated with 20 units of RNase-free DNase I (15 minutes at 37°C) and incubated with 0.1% sodium dodecyl sulfate and 0.5 mg ml⁻¹ Proteinase K (15 min at 55°C) to remove DNA and proteins, respectively. RNA was isolated from IP by PureLink RNA mini kit (Invitrogen) and quantified by reverse transcription and quantitative PCR (qPCR; primer sequences are listed in Supporting Data section, [Supporting Table S1](#)).

CHROMATIN IMMUNOPRECIPITATION ASSAYS

Chromatin immunoprecipitation (ChIP) assays were performed using the Millipore ChIP Assay Kit (catalog no.: 17-295) and antibodies for histone H3 (tri methyl K27; ab6002), H3 (Active Motif), SUZ12 (Cell Signaling Technology), and DDX5 (Millipore) were used and are listed in Supporting Data section, [Supporting Table S2](#). The sequence of primers used are listed in Supporting Data section, [Supporting Table S1](#).

IMMUNOBLOTS AND IMMUNOPRECIPITATIONS ASSAYS

Immunoblots and immunoprecipitations assays performed by standard protocols; antibodies used are listed in Supporting Data section, [Supporting Table S2](#).

REVERSE TRANSCRIPTION AND REAL-TIME qPCR

RNA was isolated using the PureLink RNA Mini Kit (12183018A; Invitrogen). Liver tissues from chronic HBV patients with HCC, tumor, and peritumoral tissue were obtained from the French National Biological Resources Centre following approved consent from the French Liver Tumor Network Scientific Committee. Complementary DNA (cDNA) was synthesized from 2.0 µg of total RNA isolated using the iScript cDNA Synthesis Kit (170-8891; Bio-Rad, Hercules, CA). Quantitative RT-PCR reactions were performed in triplicates and normalized to glyceraldehyde 3-phosphate dehydrogenase using FastStart Essential DNA Green Master (06924204001; Roche), SYBR green (Roche, Indianapolis, IN), and Roche LightCycler 96. The 2 delta delta threshold cycle (2-

ΔΔCt) method was used for analysis. Primer sequences are listed in the Supporting Data section, [Supporting Table S1](#).

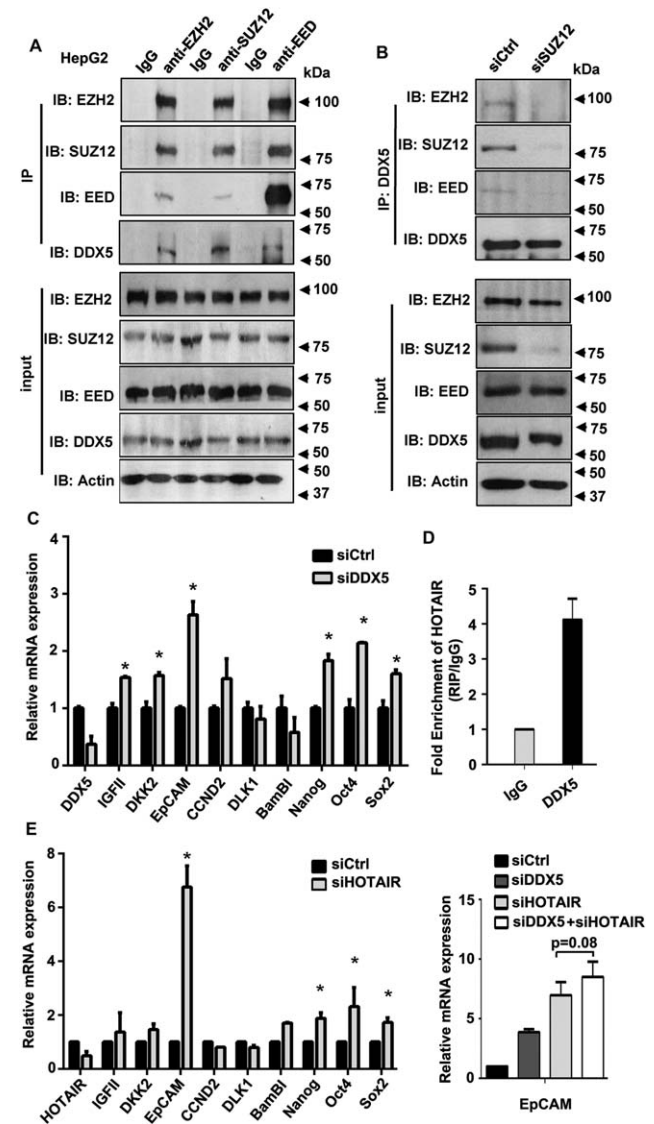


FIG. 1. DDX5 is a SUZ12 interacting protein involved in PRC2-mediated target gene repression. (A) Lysates from HepG2 cells co-immunoprecipitated (IP) with antibodies to individual PRC2 subunits, followed by immunoblot (IB) analyses with indicated antibodies (N = 3). (B) IPs of HepG2 lysates transfected with control (siCtrl) or SUZ12 (siSUZ12) siRNAs with DDX5 Ab, followed by IB with indicated Abs. (C) qPCR of indicated genes after transfection of siRNAs, control (siCtrl) or DDX5 (siDDX5), in a murine, tetracycline-regulated HBx-expressing hepatocyte cell line, the 4pX-1 cell line.⁽³⁵⁾ N = 3; error bars, SD; **P* < 0.05 using Student *t* test. (D) Association of HOTAIR with endogenous DDX5 assessed by RIP assays using IgG or DDX5 Ab and lysates from 4pX-1 cells. (E) qPCR of indicated genes in 4pX-1 cells transfected with siCtrl and HOTAIR siRNA (siHOTAIR) or combination of siHOTAIR and siDDX5 (right panel). N = 3; error bars, SD; **P* < 0.05 using Student *t* test.

STATISTICAL ANALYSIS

Statistical analysis was performed using unpaired *t* test. Differences were considered significant when $P < 0.05$. MedCalc software (Version 12.7.1.0) was used for statistical analysis of clinico-pathological patient data. Correlations were calculated by the Spearman correlation test. Log-rank test and Kaplan-Meier method were used to assess survivals. Tests were considered significant when $P < 0.05$.

Results

DDX5 IS AN SUZ12 INTERACTING PROTEIN

DDX5 was identified by mass spectrometry as an SUZ12 interacting protein (Supporting Table S3). We validated these results by immunoprecipitations of HepG2 lysates with antibodies (Abs) to each PRC2 core subunits (i.e., enhancer of zeste homolog 2 [EZH2], SUZ12, and embryonic ectoderm development [EED]; Fig. 1A and Supporting Fig. S1A). Endogenous DDX5 coimmunoprecipitated with each PRC2 subunit, showing a strong signal with SUZ12. Knockdown of SUZ12 by siRNA transfection significantly reduced coimmunoprecipitation of endogenous DDX5 with other core PRC2 subunits, suggesting that DDX5 interacts preferentially with SUZ12 (Fig. 1B and Supporting Fig. S1B). Furthermore, RNase treatment of lysates failed to disrupt DDX5/SUZ12 association, supporting that this interaction is not RNA dependent (Supporting Fig. S1C,D).

ROLE OF DDX5 IN PRC2-MEDIATED TARGET GENE REPRESSION

To determine whether DDX5/PRC2 interaction is functional, we examined the effect of DDX5 knockdown on expression of known PRC2 target genes.^(8,11) Knockdown of DDX5 in our model hepatocyte 4pX-1 cell line⁽³⁵⁾ increased expression of some, but not all, PRC2-repressed genes, including EpCAM and insulin-like growth factor II (IGFII) and pluripotency genes Nanog, octamer 4 (Oct4), and SRY (sex determining region Y)-box 2 (Sox2; Fig. 1C). Importantly, EpCAM is reexpressed in hCSCs,^(33,34) and IGFII is a known DDX5-regulated gene, serving as a positive control.⁽³⁷⁾

Given that DDX5 interacts with SUZ12 (Fig. 1A), the PRC2 complex binds HOTAIR,⁽²⁹⁾ and SUZ12

down-regulation is facilitated by HOTAIR,⁽⁹⁾ we examined whether DDX5 binds endogenous HOTAIR. RIP assays showed that DDX5 bound endogenous HOTAIR (Fig. 1D). Next, we knocked down HOTAIR by siRNA transfection in 4pX-1 cells and observed enhanced EpCAM expression, quantified by RT-PCR (Fig. 1E) and verified by EpCAM immunoblots (Supporting Fig. S2A). Knockdown of HOTAIR also resulted in statistically significant induction of Nanog, Oct4, and Sox2, but not IGFII and DKK2 messenger RNAs (mRNAs), suggesting that HOTAIR, in association with DDX5, is involved in PRC2-mediated repression of specific genes (Fig. 1E). Combined knockdown of HOTAIR and DDX5 did not have an additive effect on EpCAM expression, supporting that these two molecules act in the same pathway (Fig. 1E). ChIP assays showed that HOTAIR knockdown reduced SUZ12 occupancy at the EpCAM, Nanog, Oct4, and Sox2 promoters (Supporting Fig. S2C), but not delta-like 1 homolog and cyclin D2 promoters (Supporting Fig. S2B). Taken together (Fig. 1), these results identify DDX5 and HOTAIR as necessary partners for PRC2-mediated transcriptional repression of specific genes.

DDX5 IS DOWN-REGULATED IN HBV-INDUCED HCCs AND HBV-REPLICATING CELLS

Next, we examined DDX5 mRNA expression in liver tumors from the HBx/c-myc animal model of HBV-mediated hepatocarcinogenesis.⁽²⁾ We observed statistically significant reduction in DDX5 mRNA levels in liver tumors versus normal liver (Fig. 2A). Interestingly, DDX5 expression was also significantly reduced in group A of human liver tumors from chronically HBV-infected patients compared to peritumoral tissue (Fig. 2B).

Given that chronic HBV infection is linked to HCC pathogenesis, we reasoned that cellular mechanisms deregulated during HBV-induced hepatocarcinogenesis must provide an advantage for viral growth. Accordingly, we examined DDX5 protein levels in HBV replicating cells. We employed lysates from the HBV replication model of HepAD38 cells,⁽³⁸⁾ HBV infection models of HepG2-NTCP cells,⁽³⁹⁾ and primary human hepatocytes (PHHs)⁽⁴⁰⁾ (Fig. 2C). The HBV core (HBc) antigen is used as a marker of HBV replication (Fig. 2C), whereas quantification of viral RNA and DNA was used to monitor HBV infection in HepG2-NTCP cells (Supporting Fig. S3A). HepAD38 cells, derived from the HepG2 cell line,

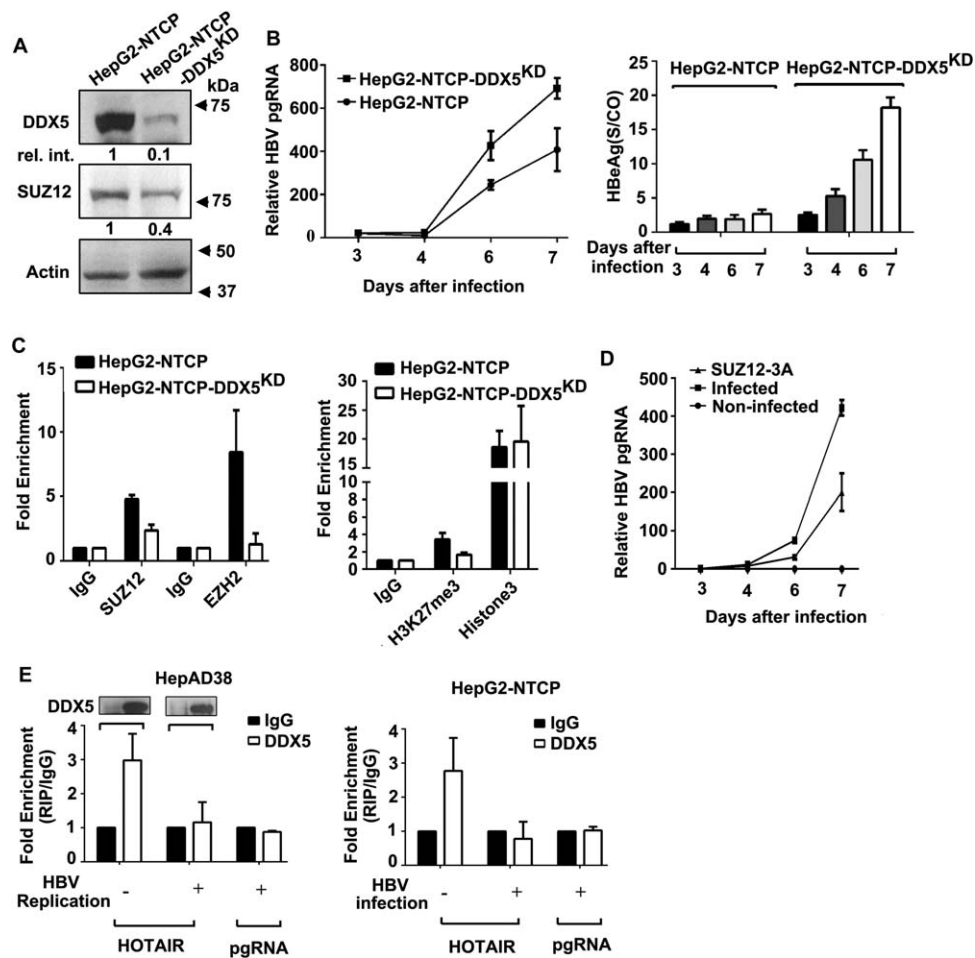


FIG. 3. DDX5 knockdown enhances HBV infection in HepG2-NTCP cells. (A) Immunoblots of DDX5 and SUZ12 using lysates from HepG2-NTCP and HepG2-NTCP-DDX5^{KD} cells. (B) HepG2-NTCP and HepG2-NTCP-DDX5^{KD} cells infected with 100 vge (virus genome equivalents) of HBV. Quantification of pgRNA by RT-PCR and HBe (S/CO = signal/cutoff) by ELISA. (C) ChIP assays of HepG2-NTCP and HepG2-NTCP-DDX5^{KD} cells with indicated Abs, on day 7 of HBV infection, using cccDNA primers.⁽⁵⁰⁾ (D) Overexpression in HBV-infected HepG2-NTCP cells of SUZ12-3A mutant: quantification of pgRNA by RT-PCR. (E) RIP assays: quantification by RT-PCR of HOTAIR binding to IgG or DDX5 in HepAD38 cells \pm HBV replication for 5 days, and HepG2-NTCP cells \pm HBV infection for 7 days. Quantification by RT-PCR of HBV pgRNA binding to IgG or DDX5 in HBV replicating (day 5) HepAD38 cells and HepG2-NTCP cells infected with HBV for 7 days. Error bars, SD.

whereas HBe levels became reduced (Fig. 2E). We interpret these results to mean that reduction of DDX5 is advantageous for viral replication.

To further confirm these results, we established the DDX5 knockdown cell line, HepG2-NTCP-DDX5^{KD} (Fig. 3A). HBV infection of HepG2-NTCP and HepG2-NTCP-DDX5^{KD} cells showed that DDX5 knockdown increased viral transcription, based on enhanced expression of pgRNA and viral HBe antigen (HBeAg), quantified by enzyme-linked immunosorbent assay (ELISA; Fig. 3B). Given that pgRNA is the template for HBV-DNA synthesis, we quantified increased total HBV DNA and cccDNA in

the presence of DDX5 knockdown (Supporting Fig. S3C). In agreement with increased pgRNA transcription in HepG2-NTCP-DDX5^{KD} cells, ChIP assays quantified reduced occupancy of SUZ12 and EZH2 associated with the viral minichromosome and reduced occupancy by H3K27me3 (Fig. 3C). By contrast, ChIP assays of SUZ12 and EZH2 at the promoters of cellular genes not targeted by the DDX5/PRC2 complex did not exhibit significant difference in their occupancy between the two cell lines (Supporting Fig. S3D). To directly link PRC2 function to transcription from the viral minichromosome, we examined the effect on HBV infection of the SUZ12 mutant

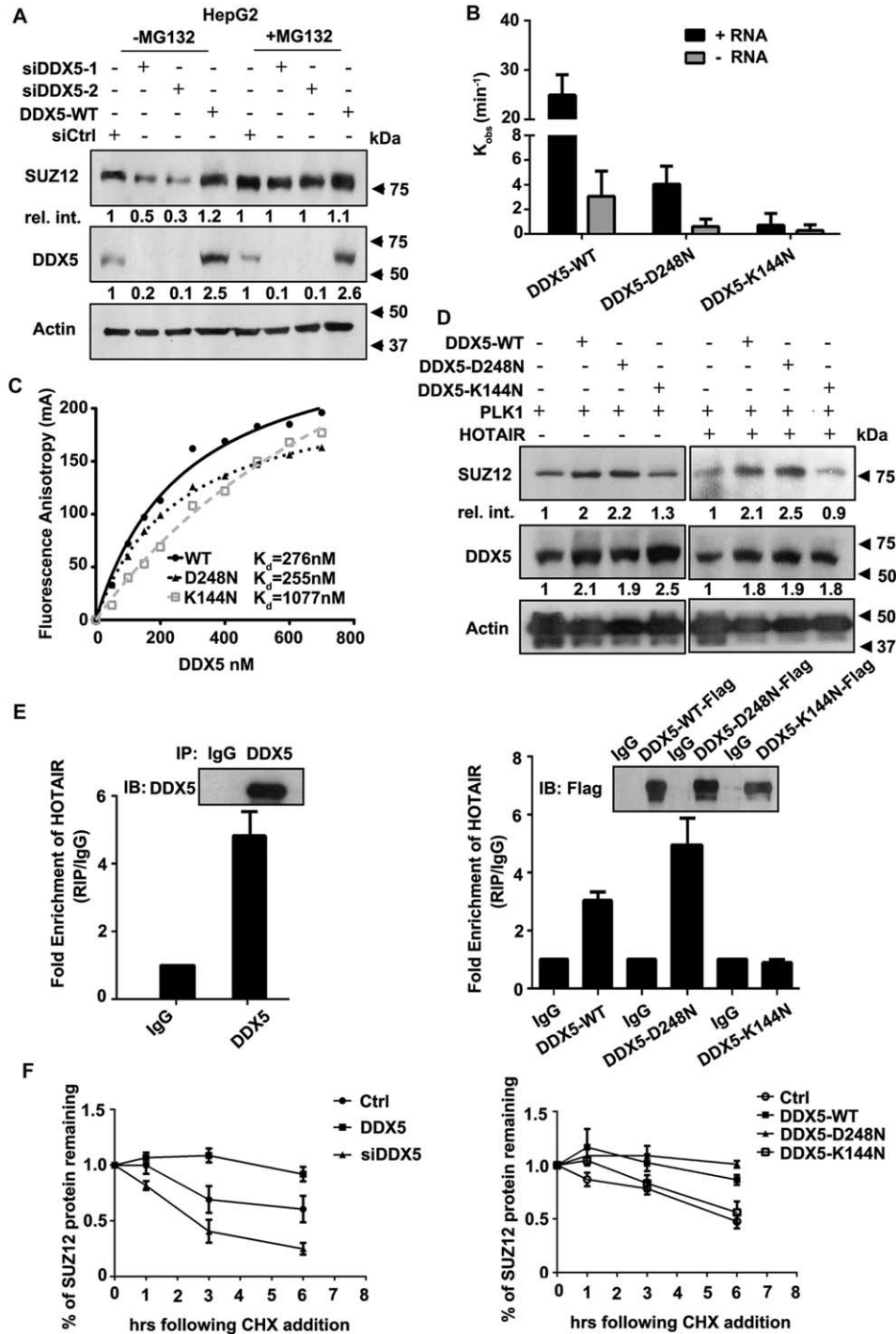


FIG. 4. DDX5 regulates SUZ12 stability. (A) Immunoblots of SUZ12 and DDX5 using lysates from HepG2 cells transfected with siRNAs for DDX5 (siDDX5-1 and siDDX5-2), control siRNA (siCtrl), or DDX5-WT plasmid, treated with \pm MG132 (10 μ M). (B) ATPase assays using 400 nM of purified, recombinant WT-DDX5 (MBP-DDX5-GST), or mutants DDX5-D248N and DDX5-K144N in the presence (+) and absence (-) of 250 μ g/mL of total yeast RNA, performed as described.⁽³⁶⁾ Error bars, SD. (C) FA assays to measure RNA-binding affinity were conducted as described⁽⁴⁴⁾ using 10 nM of 5'-FAM-labeled single-stranded RNA and increasing amount of WT-DDX5 (MBP-DDX5-GST) or tagged mutants DDX5-D248N and DDX5-K144N. (D) Immunoblots of SUZ12 and DDX5 using lysates from HEK293T cells transfected with pcDNA3 empty vector (-), DDX5-WT, DDX5-D248N, DDX5-K144N, PLK1, or HOTAIR expression vectors (all in pcDNA3). (E) RIP assays for quantification by RT-PCR of HOTAIR binding to endogenous DDX5 (left panel) and employing lysates from HEK293T cells transfected with DDX5-WT-Flag, DDX5-D248N-Flag, and DDX5-K144N-Flag vectors and immunoprecipitated with IgG or Flag Ab (right panel). N = 3, error bars, SD. (F) Quantification of SUZ12 half-life (% protein remaining), in a time course (0-6 hours) after CHX addition. siDDX5, DDX5-WT, DDX5-D248N, and DDX5-K144N encoding vectors were transfected in HEK293T cells, and CHX (20 μ g/mL) was added 24 hours after transfection. WCE were harvested 0-6 hours after CHX addition. Results represent the average from three independent experiments. N = 3; error bars, SD.

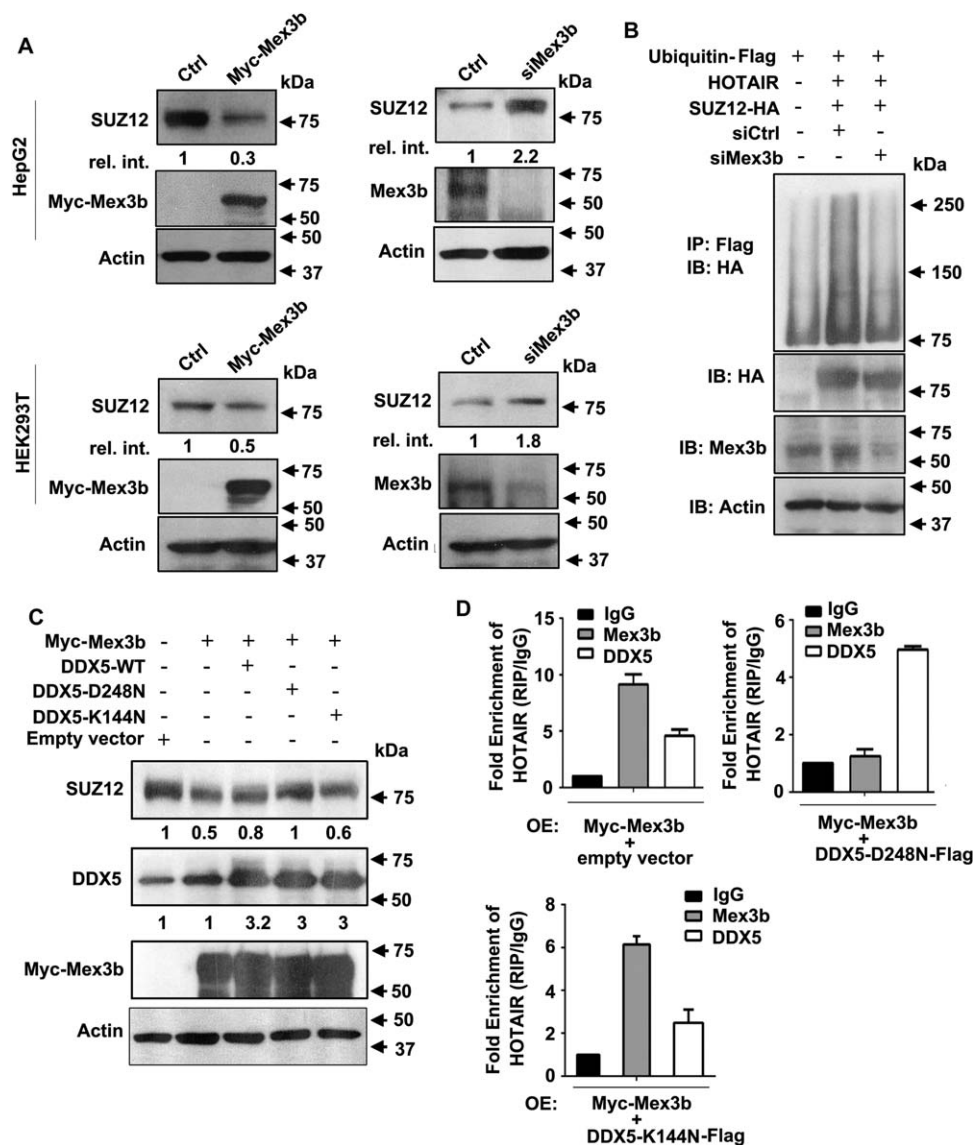


FIG. 5. Mex3b antagonizes DDX5 in SUZ12 down-regulation. (A) Immunoblots of SUZ12 and Mex3b using lysates from HepG2 (upper panels) or HEK293T (bottom panels) cells transfected with expression vector Myc-Mex3b or Mex3b siRNA (siMex3b). (B) Ubiquitination assays of SUZ12-HA in HEK293T cells cotransfected with indicated plasmids and siRNAs. WCE (0.5 mg) immunoprecipitated with hemagglutinin (HA) Ab and immunoblotted with Flag Ab. (C) Immunoblots of SUZ12, DDX5, and Mex3b using lysates from HEK293T cells transfected with expression vectors encoding Myc-Mex3b, DDX5-WT, DDX5-248N, and DDX5-K144N. (D) RIP assays for quantification by RT-PCR of HOTAIR binding to Mex3b or DDX5 with overexpressed (OE) Myc-Mex3b, in combination with empty vector, DDX5-D248N-Flag, or DDX5-K144N-Flag. RIP assays were performed using Abs for IgG, Myc epitope, or Flag. N = 3; error bars, SD.

(SUZ12-3A) that does not undergo proteasomal degradation.⁽⁹⁾ Ectopic expression of SUZ12-3A in infected HepG2-NTCP cells reduced levels of pgRNA (Fig. 3D), total HBV DNA, cccDNA, and HBeAg (Supporting Fig. S3E), supporting that PRC2-mediated repression inhibits transcription from the viral minichromosome and, in turn, HBV

replication. Interestingly, RIP assays show that in the absence of HBV replication in HepAD38 and HepG2-NTCP cells, DDX5 bound to HOTAIR (Fig. 3E). However, DDX5 association with HOTAIR was significantly reduced in the presence of HBV replication, and, notably, DDX5 did not bind viral RNA (Fig. 3E).

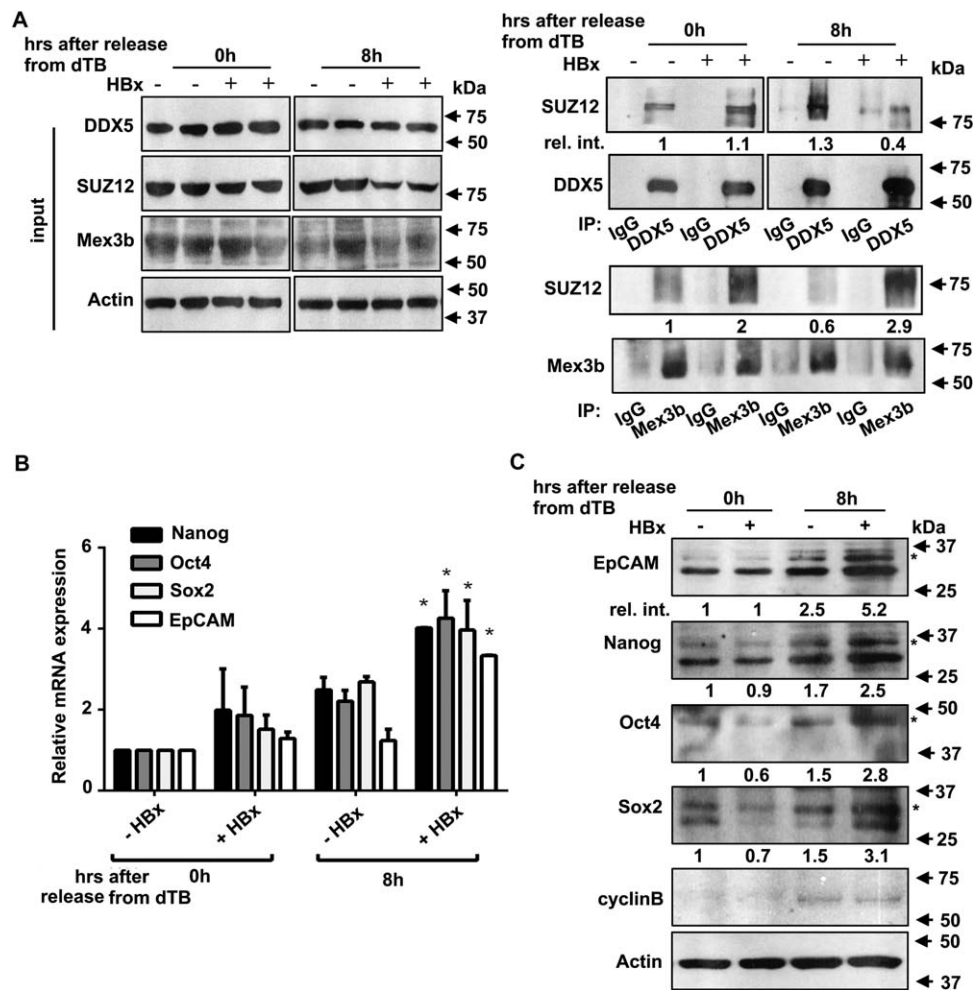


FIG. 6. HBx promotes Mex3b- and HOTAIR-mediated SUZ12 degradation during cell-cycle progression in hepatocytes. (A) 4pX-1 lysates collected at 0 (G₁ phase) and 8 hours (G₂) after release from dTB, as a function of HBx expression by tetracycline removal, were coimmunoprecipitated with DDX5 or Mex3b Abs, followed by immunoblot (IB) analyses with SUZ12 Ab. (B) RT-PCR quantification of indicated genes in 4pX-1 cells after release from dTB. N = 3; error bars, SD. P < 0.05. (C) Immunoblots of synchronized 4pX-1 lysates, ± HBx expression by tetracycline removal, with indicated Abs (N = 3).

DDX5 REGULATES SUZ12 STABILITY

We were intrigued by the concurrent reduction of DDX5 and SUZ12 protein levels in HBV-replicating cells (Fig. 2C). Given that SUZ12 undergoes proteasomal degradation,⁽⁹⁾ we examined the effect of proteasome inhibitor MG132 on SUZ12 protein levels, as a function of DDX5 depletion or overexpression in HepG2 and HEK293T cells (Fig. 4A and Supporting Fig. S4A). DDX5 knockdown reduced SUZ12 protein levels, whereas overexpression restored SUZ12 levels in the absence of MG132. By contrast, MG132 stabilized SUZ12, irrespective of DDX5

(Fig. 4A). Indeed, under conditions of SUZ12 degradation, that is, with overexpression of constitutively active PLK1 and HOTAIR,⁽⁹⁾ SUZ12 exhibited increased ubiquitination upon knockdown of DDX5, whereas DDX5 overexpression suppressed ubiquitination (Supporting Fig. S4B). By contrast, DDX5 knockdown did not affect ubiquitination of the SUZ12-3A mutant that cannot be phosphorylated by PLK1⁽⁹⁾ to initiate its proteasomal degradation (Supporting Fig. S4C).

To determine whether the DDX5 effect on SUZ12 stability was dependent on its enzymatic activity, we utilized two DDX5 mutants, DDX5-K144N and DDX5-D248N.^(41,42) To date, only the ATPase activity of

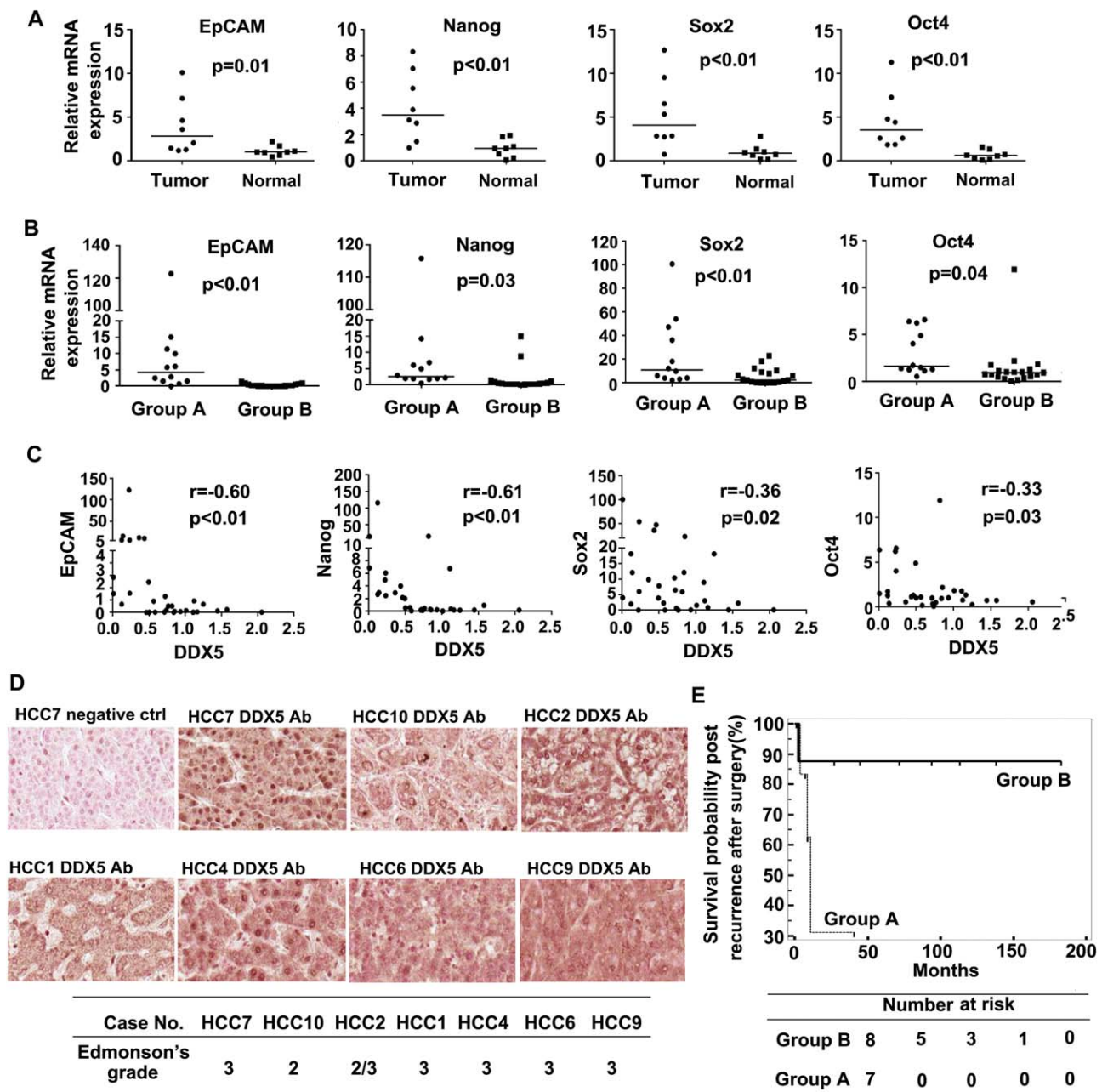


FIG. 7. Quantification of mRNA levels of EpCAM and pluripotency genes. (A) In HBx/c-myc liver tumors versus normal liver. (B) Quantification of EpCAM and pluripotency gene expression in liver tumors from chronically infected HBV patients with HCC, comparing group A versus group B from Fig. 2B. (C) Scatterplots of mRNA levels of DDX5 versus those of EpCAM or pluripotency genes in HBV-related HCCs. (D) Immunohistochemistry of human HBV-related HCCs using DDX5 Ab. (E) Kaplan-Meier curves for overall survival analysis of patients with HBV-related HCCs from group A versus group B. Log-rank test assessed survivals ($P=0.17$).

DDX5-K144N has been studied biochemically.⁽⁴³⁾ Here, using purified recombinant DDX5 proteins (Supporting Fig. S5A), we determined the ATPase and RNA-binding activity of these DDX5 mutants (Fig. 4B,C). *In vitro* ATP hydrolysis assays demonstrated that

the K144N mutation (in Walker A motif) abolished ATPase activity (Fig. 4B). In contrast, the D248N mutant (in Walker B motif) retained some RNA-dependent ATPase activity, albeit with a ~6-fold reduced k_{obs} . Consistently, RNA binding quantification

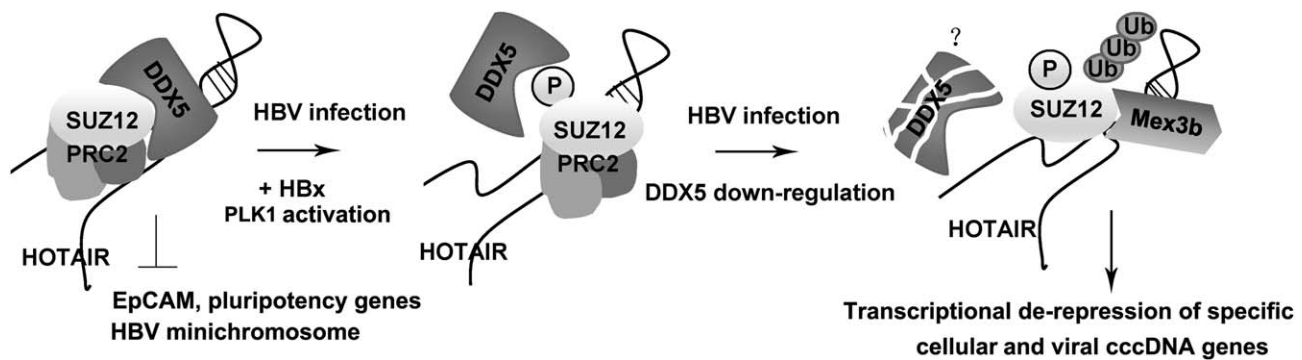


FIG. 8. Model. The DDX5/PRC2/HOTAIR complex represses transcription of specific genes. Upon expression of HBx in HBV-infected cells, HBx-mediated activation of PLK1⁽¹⁰⁾ phosphorylates SUZ12 in G₂ phase,⁽⁹⁾ resulting in DDX5 down-regulation by an unknown mechanism, indicated by the question mark (“?”), and preferential association of HOTAIR with Mex3b, a HOTAIR-binding E3 ligase.⁽³⁰⁾ Mex3b ubiquitinates SUZ12 leading to its proteasomal degradation. This results in transcriptional reactivation of PRC2/HOTAIR target genes, including EpCAM, pluripotency genes, and HBV cccDNA-encoded genes.

by FA⁽⁴⁴⁾ showed that DDX5-D248N retained RNA-binding affinity at levels similar to WT-DDX5, whereas DDX5-K144N exhibited nearly 4-fold reduced binding affinity (Fig. 4C). These results are consistent with effects of similar mutations in Walker A and B motifs of other DEAD-box proteins, suggesting that K144N abolishes ATP binding (and thus hydrolysis and ATP-dependent RNA binding), whereas D248N retains ATP and RNA-binding but is less efficient at hydrolysis.

Next, we examined the effect of wild-type (WT) and mutant DDX5 proteins on SUZ12 levels, under conditions of SUZ12 degradation, that is, with overexpression of constitutively active PLK1 and HOTAIR. WT-DDX5 and DDX5-D248N increased SUZ12 protein levels by more than 50%, whereas DDX5-K144N, which cannot hydrolyze ATP and cannot bind RNA (Fig. 4B,C), did not (Fig. 4D). These DDX5 mutants had the same effect on SUZ12 levels in the context of HBV replication (Supporting Fig. S5B). Interestingly, RIP assays demonstrated association of endogenous DDX5 with endogenous HOTAIR (Fig. 4E). Furthermore, a 5-fold increased enrichment of HOTAIR was quantified with transfected DDX5-D248N mutant versus DDX5-K144N (Fig. 4E), consistent with their demonstrated enzymatic activities (Fig. 4B,C).

To directly demonstrate the role of DDX5 and HOTAIR on SUZ12 degradation, we quantified the half-life ($t_{1/2}$) of SUZ12 after treatment with cyclohexamide (CHX). Upon knockdown of DDX5, $t_{1/2}$ of SUZ12 was quantified as 2.5 hours, in comparison to $t_{1/2} > 6$ hours with overexpression of DDX5 (Fig. 4F and Supporting Fig. S5C). Likewise, overexpression of

DDX5-D248N enhanced SUZ12 stability, whereas DDX5-K144N mutant had no effect (Fig. 4F and Supporting Fig. S5D). We conclude that DDX5-mediated stabilization of SUZ12 involves its helicase activity, evidenced by the distinct effects of DDX5-K144N versus DDX5-D248N.

HOTAIR-BINDING E3 LIGASE Mex3b ANTAGONIZES DDX5 IN SUZ12 STABILIZATION

HOTAIR functions both in PRC2-mediated gene repression⁽²⁹⁾ and protein ubiquitination and degradation by associating with RNA binding E3 ligases Mex3b and DAZ-interacting zinc finger protein 3 (Dzip3).⁽³⁰⁾ Because Dzip3 is localized in the cytoplasm,⁽³⁰⁾ we focused our studies on nucleus-localized Mex3b as a likely E3 ligase ubiquitinating nuclear SUZ12. Overexpression of Mex3b in HepG2 or HEK293T cells decreased SUZ12 levels, whereas knockdown of Mex3b by siRNA transfection increased SUZ12 protein levels (Fig. 5A). Furthermore, knockdown of Mex3b reduced SUZ12 ubiquitination (Fig. 5B). Coexpression of WT-DDX5 or DDX5-D248N, but not DDX5-K144N, antagonized the Mex3b effect on SUZ12 protein levels (Fig. 5C). To determine whether HOTAIR is involved in the antagonism between DDX5 and Mex3b, we carried out RIP assays using Abs to IgG, Myc epitope, or Flag. HOTAIR binding to Myc-Mex3b increased by 2-fold in the presence of endogenous DDX5 (Fig. 5D). By contrast, coexpression of DDX5-D248N-Flag and Myc-Mex3b led to significant reduction in HOTAIR

binding to Myc-Mex3b, whereas HOTAIR exhibited more than 4-fold increased binding to DDX5-D248N-Flag. These results demonstrate antagonism between DDX5 and Mex3b in regulating SUZ12 stability, by binding HOTAIR.

HBx PROMOTES Mex3b- AND HOTAIR-MEDIATED SUZ12 DEGRADATION DURING CELL CYCLE PROGRESSION IN HEPATOCYTES

HBx induces proteasomal degradation of SUZ12 in a cell-cycle- and PLK1-dependent manner,⁽⁹⁾ shown in the tetracycline-regulated HBx-expressing murine hepatocyte 4pX-1 cell line.⁽³⁵⁾ To determine whether cell-cycle down-regulation of SUZ12 involves antagonism between DDX5 and Mex3b for HOTAIR binding, 4pX-1 cells were synchronized in G₁/S by dTB, lysates collected at 0 (G₁ phase) and 8 hours (G₂) after release from dTB, and as a function of HBx expression by tetracycline removal.⁽¹⁰⁾ In G₂ phase, the amount of SUZ12 that coimmunoprecipitated with DDX5 was reduced by 70% in the presence of HBx, whereas Mex3b coimmunoprecipitated nearly 80% of SUZ12 (Fig. 6A). Under the same conditions, the amount of HOTAIR bound to endogenous DDX5 or Mex3b was quantified by RIP assays (Supporting Fig. S6A). As cells progressed from G₁ to G₂ in the presence of HBx, the amount of HOTAIR bound to DDX5 decreased by nearly 3-fold, whereas the amount of HOTAIR bound to Mex3b increased (Supporting Fig. S6A). Sequential ChIP assays using SUZ12 Ab followed by tandem immunoprecipitation with DDX5 Ab showed decreased SUZ12 and DDX5 occupancy at the EpCAM promoter as cells progressed to G₂ in the presence of HBx (Supporting Fig. S6B). Likewise, the silencing modification, H3K27me₃, mediated by PRC2 was also decreased in G₂ phase with HBx expression (Supporting Fig. S6C), whereas expression of EpCAM, Nanog, Oct4, and Sox2 increased, as quantified by RT-PCR (Fig. 6B) and detected by immunoblots (Fig. 6C). Given that these genes are repressed by PRC2^(8,11) and knockdown of HOTAIR or DDX5 enhanced their expression (Fig. 1), we interpret these results to mean that in G₂ phase, Mex3b-mediated ubiquitination and proteasomal degradation of SUZ12 relieved PRC2-mediated transcriptional repression.

ROLE OF DDX5 IN HBV-MEDIATED HEPATOCARCINOGENESIS

To confirm the relevance of this mechanism *in vivo*, we quantified mRNA levels of EpCAM and pluripotency genes in HBx/c-myc liver tumors, demonstrating statistically significant increase in their expression versus normal liver (Fig. 7A). To determine the clinical relevance of this mechanism, we compared expression of EpCAM and pluripotency genes in liver tumors from chronically HBV-infected patients (group A) expressing 2-fold less DDX5 mRNA versus group B (from Fig. 2B). Statistically significant induction of these genes was observed in group A tumors with 2-fold less DDX5 mRNA (Fig. 7B). Additionally, statistically significant negative correlation (*r* value) was quantified between mRNA levels of DDX5 versus those of EpCAM or pluripotency genes in HBV-related HCCs (Fig. 7C). Interestingly, Fisher's exact test also showed a negative correlation (*r* = -0.49) between low DDX5 expression (less than 2-fold vs. peritumoral tissue) and presence of well-differentiated tumors (*P* = 0.016), an indicator of poor prognosis. Immunohistochemistry of DDX5, using an independent cohort of HBV-related HCCs, showed reduction or absence of nuclear DDX5 immunostaining in poorly differentiated Edmonson's grade 3 tumors (Fig. 7D), thereby validating our observations regarding DDX5 levels and differentiation status of hepatocytes. Last, Kaplan-Meier survival curves demonstrated a trend for poor outcome after tumor resection for patients from group A (low DDX5 expression) versus those of group B (Fig. 7E). Taken together, these results strongly correlated reduction of DDX5 expression in HBV-related liver tumors to reexpression of the hCSC marker, EpCAM,⁽³⁴⁾ and pluripotency genes, likely linked to poor patient prognosis.

Discussion

In this study, we identified a novel epigenetic mechanism involving the RNA helicase DDX5, and its role in HBV biosynthesis and poor prognosis HBV-mediated liver cancer. We show that RNA helicase DDX5 regulates RNP complexes formed with lncRNA HOTAIR (see model, Fig. 8). First, we show that DDX5 interacts with SUZ12 (Fig. 1), the core subunit of the chromatin-modifying PRC2 complex, and, in association with HOTAIR, represses transcription of hCSC marker EpCAM⁽³⁸⁾ and pluripotency genes Nanog, Oct4, and Sox2 (Fig. 1). These results

establish, for the first time, the role of the mammalian RNA helicase, DDX5, functioning together with lncRNA HOTAIR and the PRC2 complex, in transcriptional repression of specific cellular genes.

Second, we show that DDX5 expression is reduced in liver tumors of HBx/c-myc bitransgenic mice⁽²⁾ and in a group of HBV-associated HCCs (Fig. 2). Significantly, reduced DDX5 expression is associated with reexpression of EpCAM and pluripotency genes as well as reduced patient survival after surgical resection of tumors (Fig. 7E). Furthermore, meta-analysis of transcriptomic data by Boyault et al.⁽⁴⁵⁾ showed that DDX5 expression was reduced in the G₁ subgroup of HBV-related HCCs (data not shown). G₁ tumors, associated with poor prognosis, overexpress fetal liver genes controlled by parental imprinting,⁽⁴⁵⁾ including EpCAM and IGFII. Interestingly, aberrant imprinting of IGFII in human tumor cell lines involves loss of SUZ12 protein by an unknown mechanism.⁽⁴⁶⁾ Thus, our mechanistic studies, together with clinical data, strongly suggest that DDX5 is an important player in development of poor prognosis HBV-related liver cancer.

Third, it is well established that deregulation of cellular mechanisms by viral oncoproteins confers an advantage to viral growth.⁽⁴⁷⁾ Indeed, down-regulation of DDX5 facilitates viral transcription and, in turn, HBV replication (Figs. 2 and 3). HBV-infected cells with stable DDX5 knockdown exhibited reduced PRC2 occupancy at the viral minichromosome and association with repressive H3K27me₃, resulting in increased pgRNA transcription and viral replication. Interestingly, both DDX5 and SUZ12 protein levels were reduced in the context of HBV replication. The mechanism of DDX5 down-regulation by HBV infection is presently under investigation, involving microRNA-mediated down-regulation (unpublished results). Furthermore, neither HOTAIR nor Mex3b ligase exert an effect on DDX5 stability (Supporting Fig. S7), and no significant correlation exists between HOTAIR and DDX5 expression levels in group A versus group B tumors (Supporting Fig. S8).

Fourth, we established a connection between DDX5 and SUZ12 stability, by identifying the E3 ligase that regulates SUZ12 half-life. We had shown that SUZ12 undergoes proteasomal degradation facilitated by HOTAIR, but the E3 ligase was not identified. Here, we show that HOTAIR-binding E3 ligase Mex3b ubiquitinates SUZ12. For these studies, we used key DDX5 mutants, which we characterized biochemically (Fig. 4). In particular, DDX5-D248N, which binds RNA but has significantly reduced ATPase activity, bound nearly

2-fold more HOTAIR and increased SUZ12 stability by displacing Mex3b from HOTAIR. These results directly demonstrate that the enzymatic activity of DDX5 regulates the RNP complexes formed with HOTAIR (i.e., the complex with PRC2 vs. Mex3b).

Importantly, the RNP complex comprised of DDX5/PRC2-bound HOTAIR identified a mechanism of transcriptional silencing of specific cellular genes. These include EpCAM and pluripotency genes, up-regulated in G₂ phase of HBx-expressing cells (Fig. 6), although global gene targets remain to be determined. Considering that SUZ12 undergoes degradation in G₂ phase of HBx-expressing cells,⁽⁹⁾ here we show that Mex3b, by displacing DDX5 from HOTAIR, ubiquitinates SUZ12, inducing its degradation. Thus, the interplay of RNP complexes with HOTAIR, regulated by DDX5, results in transcriptional de-repression of specific PRC2-silenced genes. Whether the enzymatic activity of DDX5 is cell-cycle regulated is unknown and presently under investigation. Furthermore, little is known about Mex3b regulation,⁽⁴⁸⁾ additional Mex3b substrates, or interaction with other lncRNAs.

Regarding expression of EpCAM and pluripotency genes in G₂ phase (Fig. 6), our results are consistent with recent studies that identified epigenetic factors acting in G₂ phase as essential for maintenance of pluripotency in human ESCs.⁽⁴⁹⁾ Specifically, it was shown that transcriptional induction of pluripotency genes occurs in G₂ phase,⁽⁴⁹⁾ as we also show herein. Notably, these mechanistic conclusions are consistent with *in vivo* and clinical data (Fig. 7), demonstrating strong negative correlation between DDX5 expression, expression of pluripotency genes, and differentiation status of HBV-induced liver tumors.

In summary, the data provided herein establish a novel epigenetic mechanism (model, Fig. 8), involving the antagonism between DDX5 and Mex3b in regulating SUZ12/PRC2 stability, by binding HOTAIR. This mutually exclusive binding to HOTAIR between the DDX5/PRC2 complex and the E3 ligase Mex3b, is deregulated by HBV infection resulting in de-repression of transcription both from the HBV minichromosome and select cellular genes expressed in hCSCs. Accordingly, our studies identify the RNA helicase DDX5, and E3 ligase Mex3b, as important cellular targets for design of novel, epigenetic therapies to combat HBV infection and poor prognosis HBV-associated liver cancer.

Acknowledgments: We thank the French National Biological Resources Centre for frozen human liver tissues,

obtained following approved consent from the French Liver Tumor Network Scientific Committee. The French Liver Tumor Network is funded by the Institut National de la Santé et de la Recherche Médicale (INSERM) and the Agence Nationale de la Recherche (ANR). We also thank the Biological Resources Center of Centre Léon Bérard for normal liver tissues obtained following approved consent and ministerial agreement; Dr. Pete E. Pascuzzi for bioinformatic analyses; Dr. R.L. Hullinger for critical reading of manuscript; and Dr. M. Billaud for Myc-Mex3b vector.

REFERENCES

- 1) Beasley RP, Hwang LY, Lin CC, Chien CS. Hepatocellular carcinoma and hepatitis B virus. A prospective study of 22 707 men in Taiwan. *Lancet* 1981;2:1129-1133.
- 2) Terradillos O, Billet O, Renard CA, Levy R, Molina T, Briand P, Buendia MA. The hepatitis B virus X gene potentiates c-myc-induced liver oncogenesis in transgenic mice. *Oncogene* 1997;14:395-404.
- 3) Madden CR, Finegold MJ, Slagle BL. Hepatitis B virus X protein acts as a tumor promoter in development of diethylnitrosamine-induced preneoplastic lesions. *J Virol* 2001;75:3851-3858.
- 4) Colombo M, Iavarone M. Role of antiviral treatment for HCC prevention. *Best Pract Res Clin Gastroenterol* 2014;28:771-781.
- 5) Llovet JM, Ricci S, Mazzaferro V, Hilgard P, Gane E, Blanc JF, et al. Sorafenib in advanced hepatocellular carcinoma. *N Engl J Med* 2008;359:378-390.
- 6) Xie B, Wang DH, Spechler SJ. Sorafenib for treatment of hepatocellular carcinoma: a systematic review. *Dig Dis Sci* 2012;57:1122-1129.
- 7) Wang WH, Studach LL, Andrisani OM. Proteins ZNF198 and SUZ12 are down-regulated in hepatitis B virus (HBV) X protein-mediated hepatocyte transformation and in HBV replication. *HEPATOLOGY* 2011;53:1137-1147.
- 8) Studach LL, Menne S, Cairo S, Buendia MA, Hullinger RL, Lefrancois L, et al. Subset of Suz12/PRC2 target genes is activated during hepatitis B virus replication and liver carcinogenesis associated with HBV X protein. *HEPATOLOGY* 2012;56:1240-1251.
- 9) Zhang H, Diab A, Fan H, Mani SK, Hullinger R, Merle P, Andrisani O. PLK1 and HOTAIR accelerate proteasomal degradation of SUZ12 and ZNF198 during hepatitis B virus-induced liver carcinogenesis. *Cancer Res* 2015;75:2363-2374.
- 10) Studach L, Wang WH, Weber G, Tang J, Hullinger RL, Malbrue R, et al. Polo-like kinase 1 activated by the hepatitis B virus X protein attenuates both the DNA damage checkpoint and DNA repair resulting in partial polyploidy. *J Biol Chem* 2010;285:30282-30293.
- 11) Bracken AP, Dietrich N, Pasini D, Hansen KH, Helin K. Genome-wide mapping of Polycomb target genes unravels their roles in cell fate transitions. *Genes Dev* 2006;20:1123-1136.
- 12) Pasini D, Bracken AP, Hansen JB, Capillo M, Helin K. The polycomb group protein Suz12 is required for embryonic stem cell differentiation. *Mol Cell Biol* 2007;27:3769-3779.
- 13) Zhao J, Ohsumi TK, Kung JT, Ogawa Y, Grau DJ, Sarma K, et al. Genome-wide identification of polycomb-associated RNAs by RIP-seq. *Mol Cell* 2010;40:939-953.
- 14) Rinn JL, Chang HY. Genome regulation by long noncoding RNAs. *Annu Rev Biochem* 2012;81:145-166.
- 15) Tsai MC, Manor O, Wan Y, Mosammamaparast N, Wang JK, Lan F, et al. Long noncoding RNA as modular scaffold of histone modification complexes. *Science* 2010;329:689-693.
- 16) Zhao J, Sun BK, Erwin JA, Song JJ, Lee JT. Polycomb proteins targeted by a short repeat RNA to the mouse X chromosome. *Science* 2008;322:750-756.
- 17) Cifuentes-Rojas C, Hernandez AJ, Sarma K, Lee JT. Regulatory interactions between RNA and polycomb repressive complex 2. *Mol Cell* 2014;55:171-185.
- 18) Davidovich C, Zheng L, Goodrich KJ, Cech TR. Promiscuous RNA binding by Polycomb repressive complex 2. *Nat Struct Mol Biol* 2013;20:1250-1257.
- 19) Sarma K, Cifuentes-Rojas C, Ergun A, Del Rosario A, Jeon Y, White F, et al. ATRX directs binding of PRC2 to Xist RNA and Polycomb targets. *Cell* 2014;159:869-883.
- 20) Linder P, Jankowsky E. From unwinding to clamping—the DEAD box RNA helicase family. *Nat Rev Mol Cell Biol* 2011;12:505-516.
- 21) Pan C, Russell R. Roles of DEAD-box proteins in RNA and RNP Folding. *RNA Biol* 2010;7:667-676.
- 22) Fuller-Pace FV. The DEAD box proteins DDX5 (p68) and DDX17 (p72): multi-tasking transcriptional regulators. *Biochim Biophys Acta* 2013;1829:756-763.
- 23) Rossow KL, Janknecht R. Synergism between p68 RNA helicase and the transcriptional coactivators CBP and p300. *Oncogene* 2003;22:151-156.
- 24) Wilson BJ, Bates GJ, Nicol SM, Gregory DJ, Perkins ND, Fuller-Pace FV. The p68 and p72 DEAD box RNA helicases interact with HDAC1 and repress transcription in a promoter-specific manner. *BMC Mol Biol* 2004;5:11.
- 25) Cloutier SC, Ma WK, Nguyen LT, Tran EJ. The DEAD-box RNA helicase Dbp2 connects RNA quality control with repression of aberrant transcription. *J Biol Chem* 2012;287:26155-26166.
- 26) Cloutier SC, Wang S, Ma WK, Petell CJ, Tran EJ. Long non-coding RNAs promote transcriptional poisoning of inducible genes. *PLoS Biol* 2013;11:e1001715.
- 27) Beck ZT, Cloutier SC, Schipma MJ, Petell CJ, Ma WK, Tran EJ. Regulation of glucose-dependent gene expression by the RNA helicase Dbp2 in *Saccharomyces cerevisiae*. *Genetics* 2014;198:1001-1014.
- 28) Cloutier SC, Wang S, Ma WK, Al Husini N, Dhoondia Z, Ansari A, et al. Regulated formation of lncRNA-DNA hybrids enables faster transcriptional induction and environmental adaptation. *Mol Cell* 2016;61:393-404.
- 29) Rinn JL, Kertesz M, Wang JK, Squazzo SL, Xu X, Bruggmann SA, et al. Functional demarcation of active and silent chromatin domains in human HOX loci by noncoding RNAs. *Cell* 2007;129:1311-1323.
- 30) Yoon JH, Abdelmohsen K, Kim J, Yang X, Martindale JL, Tominaga-Yamanaka K, et al. Scaffold function of long non-coding RNA HOTAIR in protein ubiquitination. *Nat Commun* 2013;4:2939.
- 31) Seeger C, Mason WS. Molecular biology of hepatitis B virus infection. *Virology* 2015;479-480C:672-686.
- 32) Pollicino T, Belloni L, Raffa G, Pediconi N, Squadrito G, Raimondo G, Levrero M. Hepatitis B virus replication is regulated by the acetylation status of hepatitis B virus cccDNA-bound H3 and H4 histones. *Gastroenterology* 2006;130:823-837.
- 33) Yamashita T, Forgues M, Wang W, Kim JW, Ye Q, Jia H, et al. EpCAM and alpha-fetoprotein expression defines novel prognostic subtypes of hepatocellular carcinoma. *Cancer Res* 2008;68:1451-1461.

- 34) Yamashita T, Ji J, Budhu A, Forgues M, Yang W, Wang HY, et al. EpCAM-positive hepatocellular carcinoma cells are tumor-initiating cells with stem/progenitor cell features. *Gastroenterology* 2009;136:1012-1024.
- 35) Tarn C, Bilodeau ML, Hullinger RL, Andrisani OM. Differential immediate early gene expression in conditional hepatitis B virus pX-transforming versus nontransforming hepatocyte cell lines. *J Biol Chem* 1999;274:2327-2336.
- 36) Ma WK, Cloutier SC, Tran EJ. The DEAD-box protein Dbp2 functions with the RNA-binding protein Yra1 to promote mRNP assembly. *J Mol Biol* 2013;425:3824-3838.
- 37) Yao H, Brick K, Evrard Y, Xiao T, Camerini-Otero RD, Felsenfeld G. Mediation of CTCF transcriptional insulation by DEAD-box RNA-binding protein p68 and steroid receptor RNA activator SRA. *Genes Dev* 2010;24:2543-2555.
- 38) Ladner SK, Otto MJ, Barker CS, Zaifert K, Wang GH, Guo JT, et al. Inducible expression of human hepatitis B virus (HBV) in stably transfected hepatoblastoma cells: a novel system for screening potential inhibitors of HBV replication. *Antimicrob Agents Chemother* 1997;41:1715-1720.
- 39) Ni Y, Lempp FA, Mehrle S, Nkongolo S, Kaufman C, Falth M, et al. Hepatitis B and D viruses exploit sodium taurocholate co-transporting polypeptide for species-specific entry into hepatocytes. *Gastroenterology* 2014;146:1070-1083.
- 40) Lucifora J, Arzberger S, Durantel D, Belloni L, Strubin M, Levrero M, et al. Hepatitis B virus X protein is essential to initiate and maintain virus replication after infection. *J Hepatol* 2011;55:996-1003.
- 41) Iyer RS, Nicol SM, Quinlan PR, Thompson AM, Meek DW, Fuller-Pace FV. The RNA helicase/transcriptional co-regulator, p68 (DDX5), stimulates expression of oncogenic protein kinase, Polo-like kinase-1 (PLK1), and is associated with elevated PLK1 levels in human breast cancers. *Cell Cycle* 2014;13:1413-1423.
- 42) Caretti G, Schiltz RL, Dilworth FJ, Di Padova M, Zhao P, Ogryzko V, et al. The RNA helicases p68/p72 and the noncoding RNA SRA are coregulators of MyoD and skeletal muscle differentiation. *Dev Cell* 2006;11:547-560.
- 43) Jalal C, Uhlmann-Schiffler H, Stahl H. Redundant role of DEAD box proteins p68 (Ddx5) and p72/p82 (Ddx17) in ribosome biogenesis and cell proliferation. *Nucleic Acids Res* 2007;35:3590-3601.
- 44) Liu X, Chen Y, Fierke CA. A real-time fluorescence polarization activity assay to screen for inhibitors of bacterial ribonuclease P. *Nucleic Acids Res* 2014;42:e159.
- 45) Boyault S, Rickman DS, de Reynies A, Balabaud C, Rebouissou S, Jeannot E, et al. Transcriptome classification of HCC is related to gene alterations and to new therapeutic targets. *HEPATOLOGY* 2007;45:42-52.
- 46) Li T, Chen H, Li W, Cui J, Wang G, Hu X, et al. Promoter histone H3K27 methylation in the control of IGF2 imprinting in human tumor cell lines. *Hum Mol Genet* 2014;23:117-128.
- 47) Dayaram T, Marriott SJ. Effect of transforming viruses on molecular mechanisms associated with cancer. *J Cell Physiol* 2008;216:309-314.
- 48) Courchet J, Buchet-Poyau K, Potemski A, Bres A, Jariel-Encontre I, Billaud M. Interaction with 14-3-3 adaptors regulates the sorting of hMex-3B RNA-binding protein to distinct classes of RNA granules. *J Biol Chem* 2008;283:32131-32142.
- 49) Gonzales KA, Liang H, Lim YS, Chan YS, Yeo JC, Tan CP, et al. Deterministic restriction on pluripotent state dissolution by cell-cycle pathways. *Cell* 2015;162:564-579.
- 50) Lucifora J, Xia Y, Reisinger F, Zhang K, Stadler D, Cheng X, et al. Specific and nonhepatotoxic degradation of nuclear hepatitis B virus cccDNA. *Science* 2014;343:1221-1228.

Supporting Information

Additional Supporting Information may be found at onlinelibrary.wiley.com/doi/10.1002/hep.28698/supinfo.